J. Phys. A: Math. Gen. 25 (1992) 6087–6098. Printed in the UK

A double chain system with varying interchain potential

Kyle Forinash and John Keeney

Natural Science Division, Indiana University Southeast, New Albany, IN 47150, USA

Received 1 June 1992

Abstract. We extend numerical investigations of the mechanics of a simple lattice model of DNA. The model consists of two linear mass chains connected by a Morse potential representing the hydrogen bonding between the sugar–phosphate backbones. Effects of variations in the Morse potential parameters on propagating breather type solutions are studied.

1. Introduction

In two earlier papers the dynamics of a system consisting of two coupled chains of masses representing a simple model of DNA were investigated [1, 2]. In this model the coupling along the chain is linear whereas the interchain coupling is determined by the nonlinear Morse potential. The motivation for including nonlinear forces in studying such a system is the observation that biological organisms overcome normal dissipative processes in order to grow and reproduce. One of the interesting phenomena seen in nonlinear dynamical systems is the self-focusing of energy with the existence of long-lived dynamic coherent structures. It is this property that has led to various attempts to apply nonlinear dynamics to biological systems, particularly DNA [3–9]. A phenomena of particular interest is the 'breathing' of DNA molecules whereby a strand of the DNA double chain opens into two separate chains for short stretches along the chain. This phenomena is well known experimentally and occurs spontaneously at (apparently) random sites along the molecule for brief periods [10]. The connection (if any) with the opening of DNA which occurs during the replication process is not well understood.

In section 2 of this paper the details of the model are reviewed. 'Breather' solutions for a semi-discrete limit for this model using the technique outlined by Remoissenet [11] are considered in section 3 and are used as initial conditions in the present study. The effects of a varying substrate potential for a single chain with nonlinear coupling which supports kink type solutions has been examined by Peyrard and Remoissenet [12, 13]. The effects of variations of the strength of the Morse potential on the initial condition breather solutions on a double chain are examined in section 4 of the present paper. The final section summarizes the results of the previous sections and notes possible implications for biological systems.

2. The model

The model under investigation consists of two chains of masses connected by linear springs along their length with the addition of nonlinear coupling between masses of

0305-4470/92/226087+12$07.50

each chain. The Hamiltonian for the system is

$$H = \sum_n 1/2m(u_n'^2 + w_n'^2) + 1/2k[(u_n - u_{n-1})^2 + (w_n - w_{n-1})^2] + V(u_n - v_n) \tag{1}$$

where u is the top chain displacement from equilibrium and w is the bottom chain displacement [1]. The corresponding velocities are v' and w'. Here k represents the linear coupling strength along the top and bottom chains. The Morse potential was chosen to represent the (multiple) interchain hydrogen bonding for the model DNA:

$$V(u_n - w_n) = D\{\exp[-a(u_n - w_n)] - 1\}^2. \tag{2}$$

By changing variables to $x_n = (u_n + w_n)/\sqrt{2}$ and $y_n = (u_n - w_n)/\sqrt{2}$ the Hamiltonian separates into in-phase and out-of-phase components where only the out-of-phase motion stretches the hydrogen bond. In-phase motion was not investigated in the present work. The equation for out-of-phase motion is

$$m\,\partial^2 y_n/\partial t^2 - k(y_{n+1} + y_{n-1} - 2y_n) - 2\sqrt{2}Da\exp(-\sqrt{2}ay_n)[\exp(-\sqrt{2}ay_n) - 1] = 0. \tag{3}$$

All figures shown were generated by time stepping through the integration of the full equations of motion for the connected chains using a fifth-order Runge–Kutta method [14]. For the symmetric initial conditions studied here this is equivalent to solving the in-phase equation of motion, equation (3). Energies were calculated directly from the model and were conserved in all cases to better than 0.001%. The masses are constrained to move only in the vertical direction and the ends of the chains were left free in order to more accurately reflect biological conditions. The effect of also including longitudinal motion has been examined by Muto *et al* [15].

3. Solutions

The Hamiltonian (1) above leads, in leading nonlinear order and using a multiple-scale expansion method, to a nonlinear Schrödinger equation with discrete breather solitary waves of the form

$$y_n(t) = \varepsilon A\,\mathrm{sech}\,\chi\cos(Knl - \Omega t) - 2\alpha\varepsilon^2 A^2\,\mathrm{sech}^2\chi + (\alpha\varepsilon^2/3)\,\mathrm{sech}^2\chi\cos[2(Knl - \Omega t)]/[3 + (16k/\omega_0^2)\sin^4(\kappa l)] \tag{4}$$

as shown by Remoissenet [11]. The motivation for the term breather is readily apparent in figure 1.

Here

$$A = [(u_e^2 - 2u_e u_c)/2PQ]^{1/2} \tag{5a}$$

$$\chi = \varepsilon(nl - V_e t)/L_e \tag{5b}$$

$$\Omega = (\varepsilon u_e/2P)(V_g + \varepsilon u_c)^{1/2} + \omega \tag{5c}$$

$$K = \kappa + \varepsilon(u_e/2P) \tag{5d}$$

$$P = (kl^2/2m\omega)[\cos(\kappa l) - (k/m\omega^2)\sin^2(\kappa l)] \tag{5e}$$

$$Q = (\omega_0^2/2\omega)\{4\alpha^2 - 2\alpha^2/[3 + (16k/m\omega_0^2)\sin^4(\kappa l/2)] - 3\beta\} \tag{5f}$$

$$\omega^2 = \omega_0^2 + 4(k/m)\sin^2(\kappa l/2) \tag{5g}$$

$$\omega_0^2 = 4Da^2/m \tag{5h}$$

$$\alpha = -6\sqrt{2}a/\varepsilon \tag{5i}$$

$$\beta = 7a^2/3\varepsilon^2. \tag{5j}$$

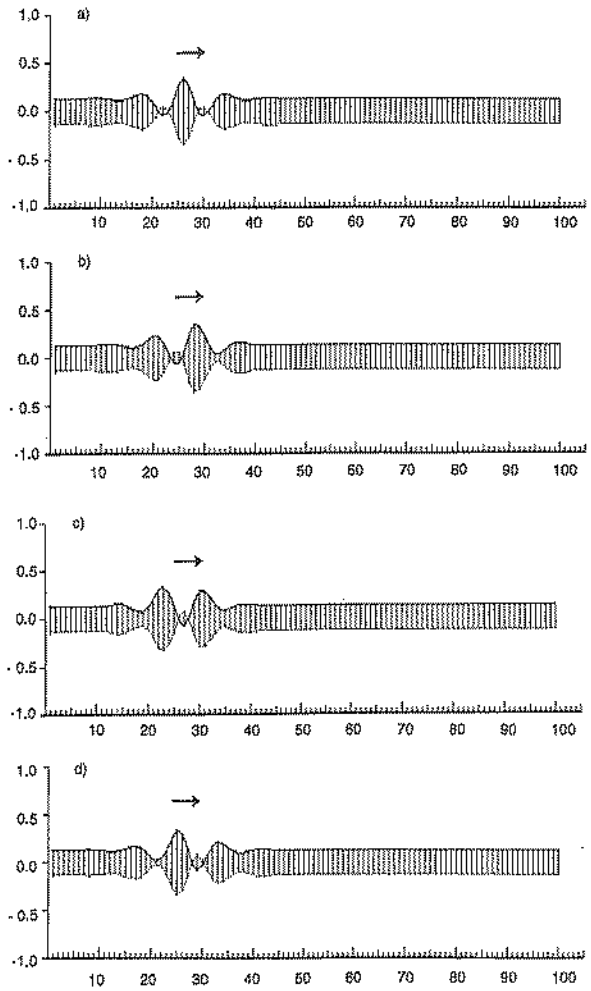

Figure 1. Time sequence of an unperturbed breather at time intervals of 0.4 time units. The initial separation distance is arbitrary and set at 0.25 units. Overlap of top and bottom chain is only apparent. Here $D = 1$, $\kappa = 0.9$, $a = 1.1$ and $k = 1$. The base pair number is on the horizontal axis and relative displacement on the vertical axis here and in subsequent figures.

Here $V_g = (kl/m\omega)\sin(\kappa l/2)$ is the group velocity, $L_e = 2P/(u_e^2 - 2u_e u_c)^{1/2}$, is the breather width, l is the lattice spacing, κ is the linear carrier wave vector, u_e is the envelope velocity, u_c is the carrier wave velocity and ε is an arbitrary scaling parameter which controls the (coupled) amplitude and width of the breather. The parameters a, D and k determine the strength of the coupling.

These breather solutions were used as initial conditions in numerical simulation experiments and found to be reasonably stable for a wide range of coupling parameters. Values of D which were investigated in the present work ranged from $D = 0.1$ to $D = 3.5$. Values of other parameters were chosen to provide the most stable pulse shape over time when undisturbed, typically $a = 1.1$, $\varepsilon = 0.01$, $k = 1$ and $\kappa = 0.9$. This choice of parameters also avoids the problem of breathers which are so narrow as to be affected by discrete lattice pinning effects which were not examined.

4. Numerical results

The precise effects on the strength of the hydrogen bonds caused by variations in the base pair pattern along a DNA chain have not been investigated. It is also not clear what effect, if any, differences in environment, such as molecule bending or the attachment of large proteins to the chain, have on the hydrogen bonding strength. It does seem logical that variations in bond strength of some type appear along the chain giving a preference for locations of the breathing behaviour. For this reason several types of changes in bond strength along the chain were investigated in the present model. It was quickly determined that the long-term stability of the initial breather modes was very sensitive to changes in the Morse potential parameter a. A value of 1.1 was chosen for the parameter a in all trials so that stability of an undisturbed breather could be assured.

In the first set of experiments a breather was launched in a region of constant D towards a region where D changed steadily to a new constant final value. Typically the breather was started centred at molecule 25 (or 75) and travelled into a region of increasing (decreasing) D located between molecules 40 and 60 on the chain. If the increase in D is small enough, for example $D=1$ to $D=1.1$, the breather is able to go down the incline with small adjustments in shape (figure 2). A breather travelling up the incline shows reflection of some energy and the transmission of a pulse shape (figure 3). For moderate increases in D, for example $D=0.8$ to $D=1$, a greater difference appears between going up and coming down the potential gradient. Breathers can travel down the incline with changes in shape (while still coherent) but reflect off of the incline when launched towards increasing D (figure 4). The reflected breather has the identical shape of the launched breather but travels in the opposite direction. When the change in D is quite large ($D=0.6$ to $D=1.2$) the breather reflects when approaching from both the low side and the high side of the D gradient region. When approaching from the high side there is some radiation which continues in the decreas-

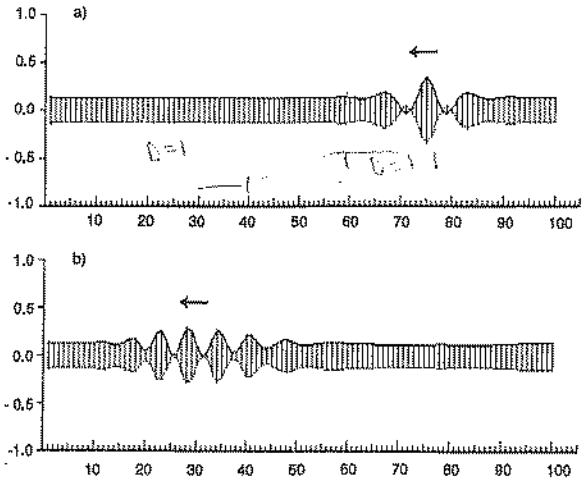

Figure 2. Time sequence of a breather (moving in the direction of the arrow) at (*a*) $t=0$ and (*b*) $t=144.4$ time units. $D=1$ for molecule numbers <40, $D=1.1$ for molecule numbers >60 and D gradually increases from 1 to 1.1 between molecules 40 and 60. Here $\kappa=0.9$, $a=1.1$ and $k=1$.

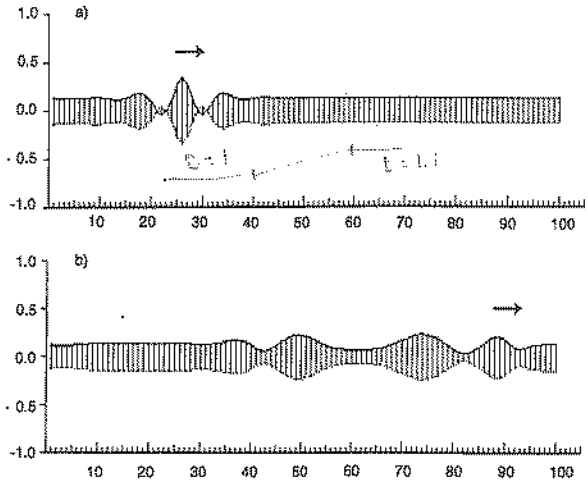

Figure 3. Time sequence of a breather (moving in the direction of the arrow) at (*a*) $t = 0$ and (*b*) $t = 240.8$ time units. $D = 1$ for molecule numbers <40, $D = 1.1$ for molecule numbers >60 and D gradually increases from 1 to 1.1 between molecules 40 and 60. Here $\kappa = 0.9$, $a = 1.1$ and $k = 1$.

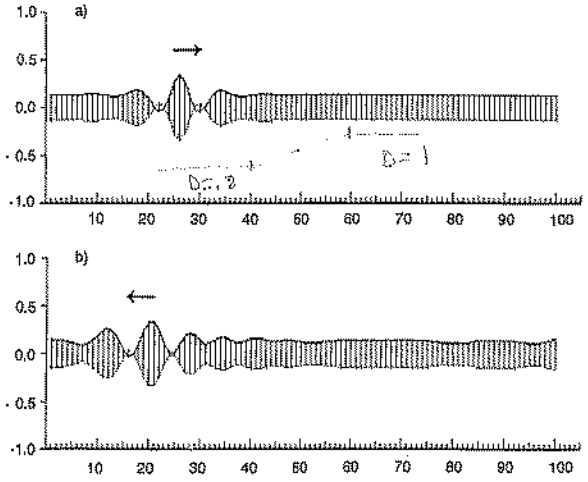

Figure 4. Time sequence of a breather (moving in the direction of the arrow) at (*a*) $t = 0$ and (*b*) $t = 241.2$ time units. $D = 0.8$ for molecule numbers <40, $D = 1$ for molecule numbers >60 and D gradually increases from 0.8 to 1 between molecules 40 and 60. Here $\kappa = 0.9$, $a = 1.1$ and $k = 1$.

ing D direction but a breather shape very similar to the launched shape is reflected (figure 5). A possible explanation based on energy arguments will be given below.

In the above trials the change in D was effected over a space of 20 molecules along the chain. The same change in D was made over shorter and longer distances to look for possible interacting length scales between the breather size and the incline size. For breathers travelling over a decrease in D there appears to be little difference between less steep ($D = 0.8$ to $D = 1$ over 40 molecules) and more steep ($D = 0.8$ to $D = 1$ over 5 molecules) changes. For breathers travelling towards an increase in D, the speed at which the breather reflects is affected by the steepness. A steeper change

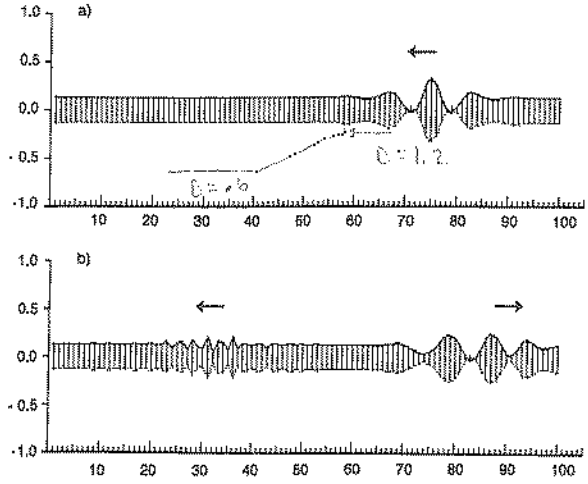

Figure 5. Time sequence of a breather (moving in the direction of the arrow) at (*a*) $t = 0$ and (*b*) $t = 140.8$ time units. $D = 0.6$ for molecule numbers <40, $D = 1.2$ for molecule numbers >60 and D gradually increases from 0.6 to 1.2 between molecules 40 and 60. Here $\kappa = 0.9$, $a = 1.1$ and $k = 1$.

in D causes a more rapid reflection, a less steep change causes a slower turnaround. The reflected breather is the same in both cases, however.

A second set of trials involved launching a breather mode on a chain with a sinusoidally varying D. Low amplitude, low frequency changes in D ($D = 1 \pm 0.04 \sin(0.03n)$ where n is the molecule number) had negligible effect on breather motion. Low amplitude, high frequency changes in D ($D = 1 \pm 0.04 \sin(0.16n)$ where n is the molecule number) had slight effects on breather motion, causing some radiation (figure 6). The phase (the + or − sign in front of the sine) of the variation in D had no effect in these trials.

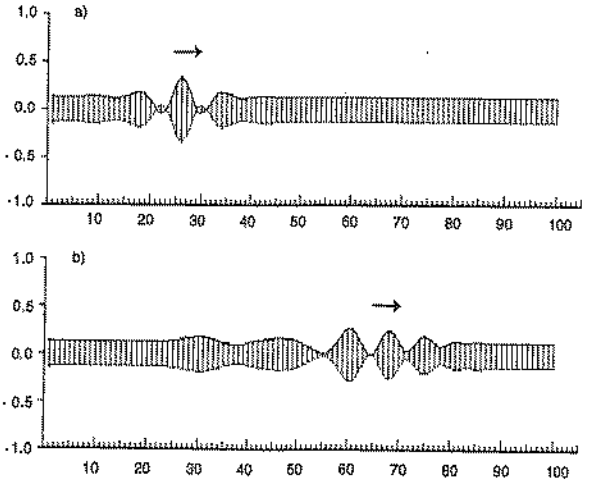

Figure 6. Time sequence of a breather (moving in the direction of the arrow) at (*a*) $t = 0$ and (*b*) $t = 143.6$ time units. $D = 1 + 0.04 \sin(0.16n)$ where n is the molecule number. Here $\kappa = 0.9$, $a = 1.1$ and $k = 1$.

Large amplitude, high frequency changes in D ($D=1\pm0.6\sin(0.16n)$ where n is the molecule number) trapped breathers and modified their shape somewhat (figure 7). Phase was not a factor for these cases. Phase did have an effect for large amplitude, low frequency changes. If the breather was launched centred near a maximum in D ($D=1+0.6\sin(0.03n)$ and breather centred at 25) it remained trapped with shape changes. If the breather was launched centred near a minimum in D ($D=1-0.6\sin(0.03n)$ and breather centred at 25) it propagated with shape changes and some radiation (figure 8).

In a subsequent set of experiments, breathers were launched so as to interact with a region where D changed gradually from a value of 1 to another value (either larger or smaller) and then back to 1. Two shapes were investigated in this set of trials; a

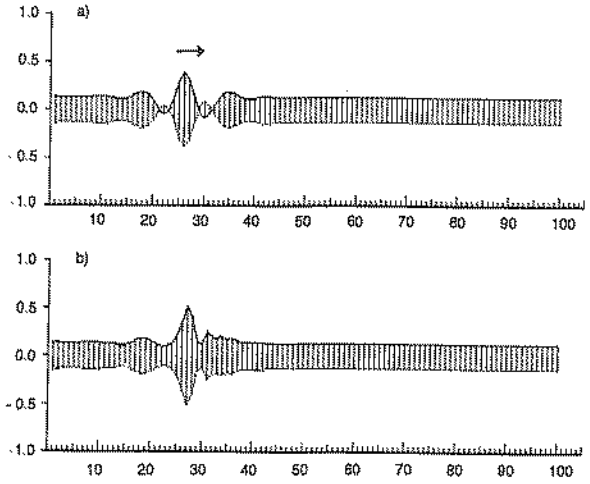

Figure 7. Time sequence of a breather (moving in the direction of the arrow) at (*a*) $t=0$ and (*b*) $t=144.4$ time units. $D=1+0.6\sin(0.16n)$ where is the molecule number. Here $\kappa=0.9$, $a=1.1$ and $k=1$.

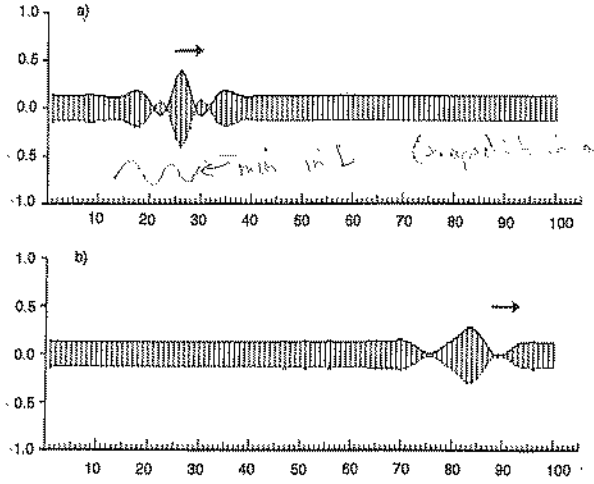

Figure 8. Time sequence of a breather (moving in the direction of the arrow) at (*a*) $t=0$ and (*b*) $t=142.8$ time units. $D=1-0.6\sin(0.03n)$ where n is the molecule number. Here $\kappa=0.9$, $a=1.1$ and $k=1$.

sawtooth shape consisting of a linear increase (or decrease) followed by a linear decrease (or increase) and a hyperbolic secant shape of varying widths and heights. The effect of sawtooth shaped changes in D were identical to effects of hyperbolic secant shaped changes of comparable size and magnitude. For cases where the breather was launched towards a region where D was increased, for example $D = 1 + 0.1\ \mathrm{sech}[(n-50)/8]$ with n as the molecule number, there was always some reflection. For small positive changes in D there was also coherent transmission of energy but the transmitted pulse was more spread out than the original breather. When the change in D was positive and large, there was almost total reflection, except for very narrow variations in D (for example $D = 1 + 0.4\ \mathrm{sech}[(n-50)/0.5]$) (figure 9). In these cases the breather appeared to be split into two breathers of lesser amplitude.

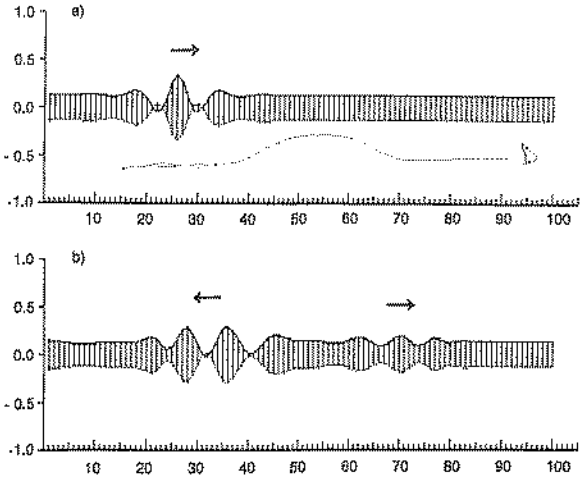

Figure 9. Time sequence of a breather (moving in the direction of the arrow) at (*a*) $t = 0$ and (*b*) $t = 140.8$ time units. $D = 1 + 0.4\ \mathrm{sech}\{(n-50)/0.5\}$ where n is the molecule number. Here $\kappa = 0.9$, $a = 1.1$ and $\kappa = 1$.

In cases where the change in D was a decrease (and subsequent increase back to the original value) the breather passed through the deformity with only minor loss of energy, regardless of the width or depth (with D always greater than zero) of the modified region.

Breathers were also launched in the deformity region, rather than outside the region travelling towards it. For all cases where the modified D was lower than surrounding regions, the breather was trapped with some shape change, regardless of the magnitude or size of the modification in D (figure 10). In the case of breathers launched in regions of positive change in D (for example $D = 1 + 0.6\ \mathrm{sech}[(n-50)/4]$) two different results were seen depending on the magnitude of the change in D. Small changes in D ($D = 1$ up to 1.6) caused a breather launched on the impurity region to split with radiation travelling off in two different directions (figure 11). If the variation in D was large, however, a rather unexpected effect was seen. For breathers launched at the centre of a region of $D = 1 + 2\ \mathrm{sech}[(n-50)/8]$, the breather remained trapped in this region. Although the shape of the breather was not conserved, the energy did not leave the region of the deformity even over very long time periods (figure 12).

A final group of trials involved the interaction of two breathers, one of which was initially trapped in a region of lower D. It was found that moving breathers pass

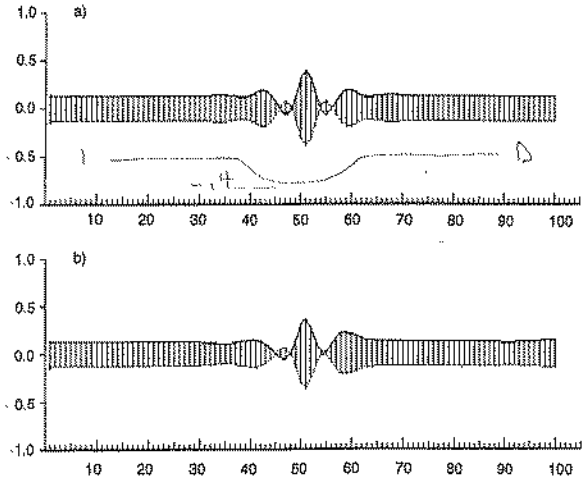

Figure 10. Time sequence of a breather (moving in the direction of the arrow) at (*a*) $t = 0$ and (*b*) $t = 199.2$ time units. $D = 1 - 0.4\,\mathrm{sech}\{(n-50)/8\}$ where n is the molecule number. Here $\kappa = 0.9$, $a = 1.1$ and $k = 1$.

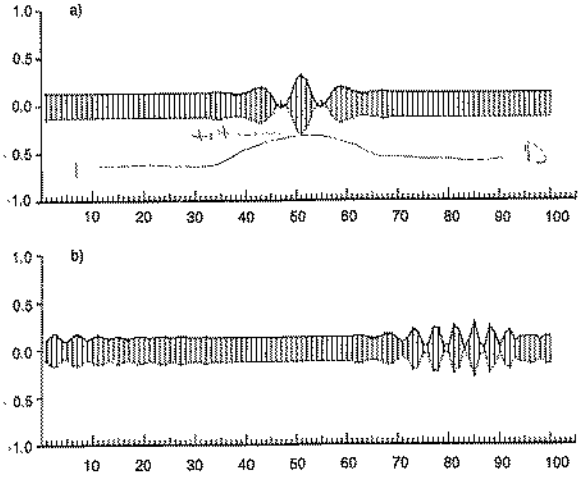

Figure 11. Time sequence of a breather (moving in the direction of the arrow) at (*a*) $t = 0$ and (*b*) $t = 190.4$ time units. $D = 1 + 0.4\,\mathrm{sech}\{(n-50)/8\}$ where n is the molecule number. Here $\kappa = 0.9$, $a = 1.1$ and $k = 1$.

through the breather trapped in the modified region the same way they pass through a modified region with no trapped breather (figure 13). Neither the trapped breather or the moving breather is disturbed.

5. Conclusion

A possible explanation of trapping in regions of larger values of D comes from energy considerations. Scharf and Bishop have examined a single chain lattice described by a particular discrete nonlinear Schrödinger equation with an added on-site potential [16, see also 17]. They show that breather solutions for that system can be treated with

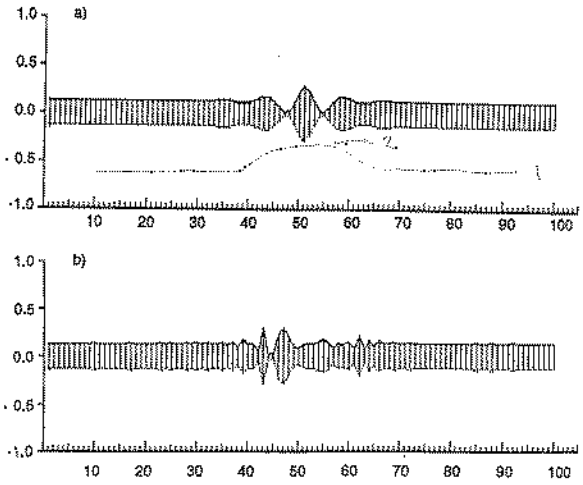

Figure 12. Time sequence of a breather (moving in the direction of the arrow) at (*a*) $t=0$ and (*b*) $t=294.0$ time units. $D=1+2\,\mathrm{sech}\{(n-50)/8\}$ where n is the molecule number. Here $\kappa=0.9$, $a=1.1$ and $k=1$.

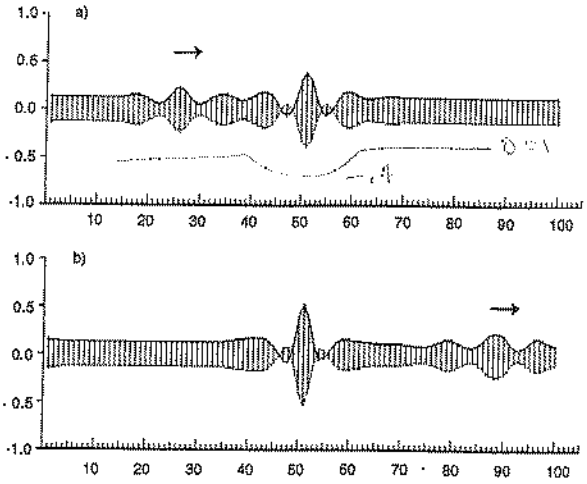

Figure 13. Time sequence of two breathers (one starting centred at molecule 25 moving in the direction of the arrow, the other trapped, centred at molecule 50) at (*a*) $t=0$ and (*b*) $t=191.6$ time units. $D=1-0.4\,\mathrm{sech}\{(n-50)/4\}$ where n is the molecule number. Here $\kappa=0.9$, $a=1.1$ and $k=1$.

a collective coordinate approach in which the breather is described as a particle interacting with an effective potential. Analyses given in that paper show that because of the way the effective potential depends on the added on-site potential, positive on-site potentials can trap breathers the same way negative on-site potentials can. The present problem is different in that rather than having an added on-site potential which varies, the parameters in the Schrödinger equation itself are changing. The analysis in terms of collective coordinates does not appear to be possible for the present case but it seems reasonable to expect similar effects.

Energy surfaces and constant energy contours are shown in figure 14 for variable D plotted against the adjustable parameters κ and ε. The adjustable parameter ε

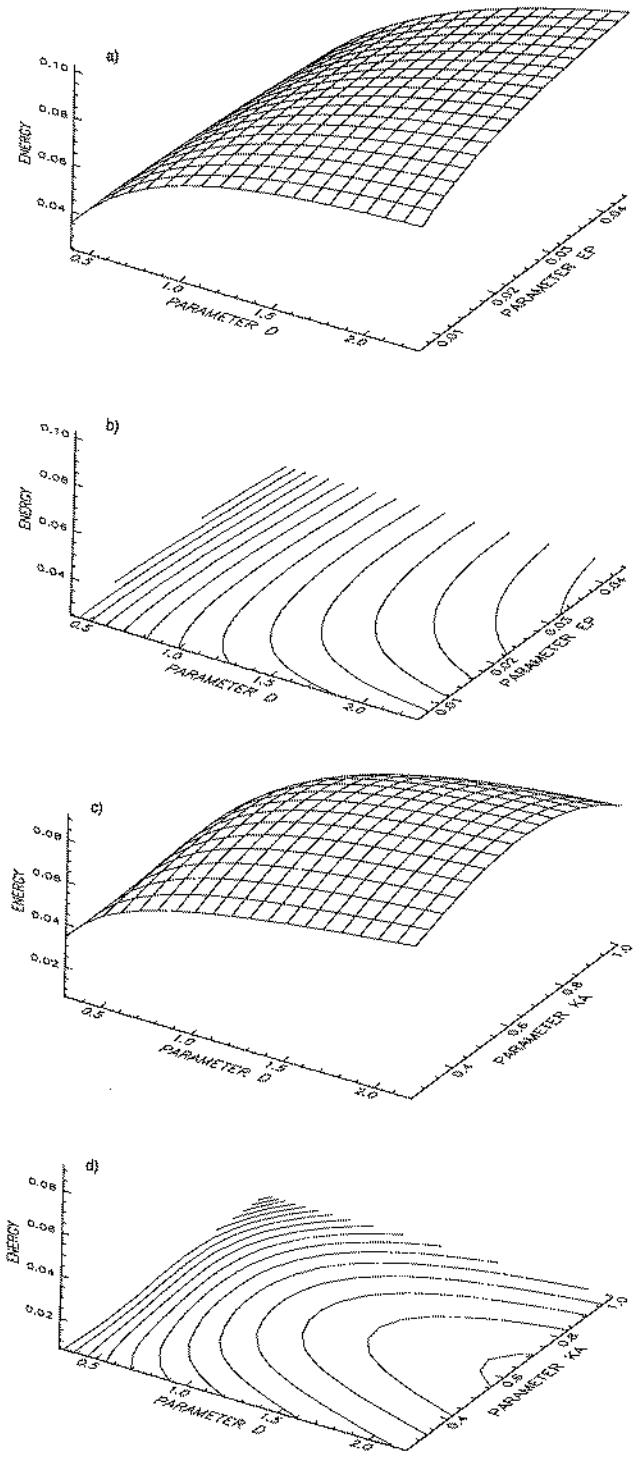

Figure 14. Plot of energy as a function of the parameters D, e and κ. D versus e (labelled *ep* in the figure) is shown in 14(a) and 14(b). The variation of D versus κ (labelled *ka* in the figure) is shown in 14(c) and 14(d).

determines the maximum amplitude and also the width of the initial breather. The carrier wave vector, κ, controls the internal shape of the breather, and consequently the speed since the initial velocities were determined from derivatives of the initial positions of the masses. Larger values of κ give higher speeds. Some values of κ give rise to other types of nonlinear pulses such as 'dark' solitons, asymmetric envelopes, etc, with imaginary amplitudes. The present model has real amplitudes which thus restricts the values of κ to the range $0 > \kappa > 1$. It is clear from the energy contour diagram in figure 14 that, for the range of parameters examined here, increasing D while trying to conserve energy would necessitate changing κ to restricted values. This accounts for the reluctance of a breather to move into regions of larger D. When moving into regions of lower D, if the change is not too abrupt, there is the possibility of having enough energy to create new breathers. One interpretation of the extra humps in figure 2(b) is that a second breather is calving off of the first because of the extra energy available.

The present double chain model is far too simple to account for many of the complicated effects seen in real DNA. Longitudinal motion along the chain, coiling resulting in possible diagonal bonding and other secondary structural effects have not been included here. However it is interesting to note from the present results that self-localized coherent breathing states are affected by small changes in potential parameters. Thus a mechanism exists whereby small inhomogeneities along the chains representing genetic coding can affect the dynamics of opening and closing of the double chain system. The present model is thus a step towards understanding some of the nonlinear dynamics which may be occurring along a DNA molecule during or preceding the processes of chain opening and closing.

Acknowledgment

The authors would like to thank David W Taylor at IUS for helpful discussions.

References

[1] Peyrard M and Bishop A R 1989 *Phys. Rev. Lett.* **62** 2755
[2] Forinash K, Bishop A R and Lomdahl P S 1991 *Phys. Rev.* B **43** 10743
[3] Englander S W, Kallenbach N R, Heeger A J, Krumhansl J A and Kitwin S 1980 *Proc. Natl Acad. Sci. USA* 777 7222
[4] Yomosa S 1983 *Phys. Rev.* A **27** 2120; 1984 *Phys. Rev.* A **30** 474
[5] Takeno S and Hommma S 1987 *Prog. Theor. Phys.* **77** 548
[6] Zhang Chun-Ting 1987 *Phys. Rev.* A **35** 886
[7] Prohofsky E W 1988 *Phys. Rev.* A **38** 1538
[8] Muto V, Scott A C and Christiansen P C 1989 *Phys. Lett.* **136A** 33
[9] Dauxois T 1991 *Phys. Lett.* **159A** 390
[10] Freifelder D 1987 *Molecular Biology* (Boston: Jones and Bartlett)
[11] Remoissenet M 1986 *Phys. Rev.* B **33** 2386
[12] Peyrard M and Remoissenet M 1982 *Phys. Rev.* B **26** 2886
[13] Remoissenet M and Peyrard M 1984 *Phys. Rev.* B **29** 3153
[14] Press W H, Flannery B P, Teukolsky S A and Vetterling W T 1989 *Numerical Recipes* (Cambridge: Cambridge University Press)
[15] Muto V, Lomdahl P S and Christiansen P L 1989 *Los Alamos preprint* LA-UR 89-4027
[16] Scharf R and Bishop A R 1991 *Los Alamos preprint*
[17] Sanchez A, Scharf R, Bishop A R and Vazquez L 1992 *Phys. Rev.* A **45** 1207